Correlations between the Scanning Tunneling Microscopy Imaged Configurations and the Electronic Structure on Stepped Si(111)-(7 × 7) Surfaces

M. Hupalo, B. J. Min,* C. Z. Wang, K. M. Ho, and M. C. Tringides
Department of Physics, Iowa State University and Ames Laboratory, Ames, Iowa 50011
(Received 8 November 1999)

We have observed the dependence of the scanning tunneling microscopy (STM) imaged atom intensity within the (7 × 7) unit cell on stepped Si(111) as a function of the tunneling voltage. Pronounced differences from the corresponding atom intensity on the flat surface are observed for the contrast of atoms on the low versus the high side of the step and for the contrast between the faulted versus unfaulted subcells of the (7 × 7) structure. These differences can be accounted for by changes in the electronic structure within the (7 × 7) subcells adjacent to the step. Calculations of the local density of states and the STM images using a tight-binding method are in excellent agreement with the experimental results.

PACS numbers: 61.16.Ch, 73.20.–r

Different methods based on the scanning tunneling microscopy (STM) have been used to obtain information about complementary aspects of the surface structure, i.e., atom positions and local electronic structure. The two aspects are closely interrelated since changes in the atom position can affect the potential experienced by the electrons and therefore the resulting electronic eigenstates; conversely spectroscopic measurements showing the presence of a new electronic state imply perturbations in the real space atomic configuration. Stepped surfaces provide good testing grounds to illustrate such interrelated effects since the presence of a step reduces the surface symmetry and increases the number of dangling bonds of the atoms at the step. The local relaxation of the step atoms to minimize the total energy of the system can redistribute the electron charge to partially satisfy the dangling bonds and can lead to corresponding electronic changes in the density of states within the subcells of the (7 × 7) unit cell. It is the purpose of this Letter to show these interrelated effects in a series of STM images we obtain on stepped Si(111)-(7 × 7) surfaces as a function of the tunneling voltage. Strong variations are found in the apparent structure and the adatom intensity within the two subcells of the (7 × 7) unit cell on either side of the step. The observed variations can be explained from changes of the local density of states of the adatoms within the two subcells of the (7 × 7) unit cell on the stepped surface with respect to the corresponding density of states within the subcells on the flat surface. Calculated images by summing up the electron density at fixed distance from the surface of all the states within the range of the tunneling voltage reproduce the experimentally observed contrast between the different subcells.

The widely accepted model of the (7 × 7) reconstruction is the dimer adatom stacking fault model proposed 15 years ago from transmission electron microscopy diffraction intensity analysis [1] and confirmed extensively with numerous techniques, including STM. The (7 × 7) unit cell is divided into two subcells, the faulted and the unfaulted, that differ in the stacking structure of the first bilayer. On the flat Si(111)-(7 × 7) surface it is known [2] that for images taken at negative polarity (i.e., the sample is biased negatively so electrons tunnel from the occupied states of the sample) the adatoms in the faulted subcell appear brighter than the adatoms in the unfaulted subcell because the local density of states of the adatoms below the Fermi level is higher in the faulted than in the unfaulted subcell. Furthermore the six adatoms at the top layer are imaged with unequal intensity (at negative bias) with the three corner adatoms (i.e., the ones closer to the corner holes) being more intense than the middle adatoms. An explanation for this uneven adatom intensity is based on charge transfer [3–6]: The middle adatoms transfer part of their electron charge to the rest adatoms at the level below (the transfer is more efficient for the middle adatoms because they have two neighboring rest atoms while the corner adatoms have only one neighboring rest atom). The possibility of charge transfer is additionally supported from the absence of this intensity variation for positively biased images (since no charge transfer is expected). For larger reconstructed unit cells ($n \times n$)-Si(111) (with $n = 9–13$) the perimeter adatoms, which have a lower number of neighboring rest atoms, appear more intense than the inside adatoms in negative bias STM images [4]. It is the purpose of this Letter to address the question whether these features of the (7 × 7) unit cell, typical of the flat surface, are different for a (7 × 7) unit cell with its two subcells on either side of a step.

The experiments were carried out in a UHV chamber of base pressure 8×10^{-11} with a 1.2° Si(111) misoriented sample in the $[\bar{1}\bar{1}2]$ direction. The sample was cleaned resistively with direct current applied in the step-up direction in accordance to Ref. [7]. After heating to 1250 °C when sublimation of Si occurs, the surface was quenched to 900 °C followed by slow cooling at a rate 0.5 °C/sec. This process resulted in a stepped surface with regularly spaced steps.

The theoretical calculations of the density of states for the different subcells and of the corresponding STM

images were performed by using the recently developed environment-dependent tight-binding potential [8] for Si that takes into account the specific bonding environment of an atom, extending realistically the normally used two-center approximation. The energy parameters in the model describing the interactions between atoms at two sites (the diagonal matrix elements, the hopping parameters, and the pairwise repulsive interactions) depend on a rescaled distance and a screening function that are modified according to the number of atoms intervening between the two interacting atoms, with the net result that local environments with larger coordination numbers are parametrized with longer bond lengths and weaker interaction strengths. This new tight-binding scheme has been very successful to explain the observed bulk properties of silicon. It is highly transferable to other geometries (surfaces, clusters) [8,9].

Stepped Si(111) surfaces have been studied previously [10–12]. It was shown that the (7×7) phase nucleates at steps after slow cooling from high temperatures [13,14]. Depending on the heating method and the cooling rate different step types form differing by the type of subcell nucleating on the high side of the step (whether it is faulted or unfaulted) and the location of the step, defined by the distance between the dimer rows nearest to the step on the high side from the corner holes on the low side of the step. This distance can take seven possible values $[(n + c)a$, where $a = 3.3$ Å $= \frac{1}{7}$ the height of the subcell triangles, n is an integer less than 7 and c is a constant equal to $\frac{2}{3}a$ $(\frac{4}{3}a)$ for the unfaulted (faulted) subcell] before an equivalent step structure is repeated. This results in a total of 14 different types of steps (seven types for faulted and seven for unfaulted subcells on the high side of the step). In our experiments we study the structure of a U2 step, i.e., a step with an unfaulted subcell on the high side and with $n = 2$, which was found to be the most probable step configuration [10].

Figures 1(a)–1(c) show images of the step running along the $[\bar{1}10]$ direction for different tunneling voltages of -0.5, -1, and $+0.25$ V, respectively, with the low side of the step to the left [which has one subcell of the (7×7)]. The subcell with its base parallel to the step direction on the high side is unfaulted, as evidenced from the lower intensity when compared to the neighboring subcell, so this step is a U type. The transition region separating the two subcells is measured to be 9.1 Å, which indicates that $n = 2$ with four extra adatoms in the transition region: three adatoms in one row and a fourth adatom forward towards the high side of the step clearly resolved, especially at negative polarity. The two subcells on the low and high sides are shifted by an amount 3.84 Å, along the step direction. The configuration of the atoms at the step is shown schematically in Fig. 2, with the size of the symbol indicating the proximity of the atom towards the surface. This structure was constructed by using the experimental STM information as a guide and was optimized by the calculations with the environment dependent Si tight-binding potential.

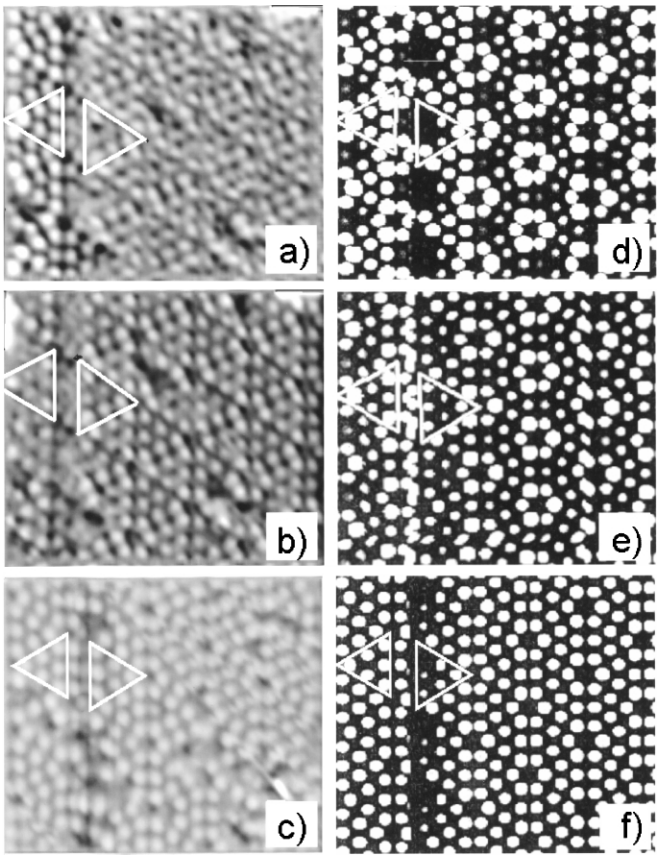

FIG. 1. Comparisons between STM images obtained at different voltages [-0.5 V (a), -1 V (b), and $+0.25$ V (c)] and corresponding theoretical calculations (d)–(f) based on the environment-dependent tight-binding Si potential. The contrast between the low and the high side of the subcells is maximum at $V = -0.5$ V as a result of changes of the adatom density of states in the different subcells adjacent to the step.

A close examination of the STM image intensity reveals some important changes as a function of the tunneling voltage. At -0.5 V the subcells on the low side have higher intensity than the subcells on the high side of the step, with the adatoms on the low side of the step observed with remarkable contrast. The difference in intensity between the faulted and unfaulted subcells is seen on the high side of the step (expected for the flat surface), but it is much reduced between the faulted and the unfaulted subcell on the low side of the step. When the tunneling voltage is increased to -1 V the difference in the intensity between the subcells on the low and the high side of the step is reduced and the adatom contrast is suppressed. In addition the contrast between the unfaulted and faulted subcells on the high side is reduced (i.e., some of the unfaulted subcells have almost the same intensity as the faulted ones). For positive polarity $V = +0.25$ V the image is dramatically different with no contrast between faulted and unfaulted subcells (on either side of the step) and no difference in intensity between the subcells on the low and the high side of the

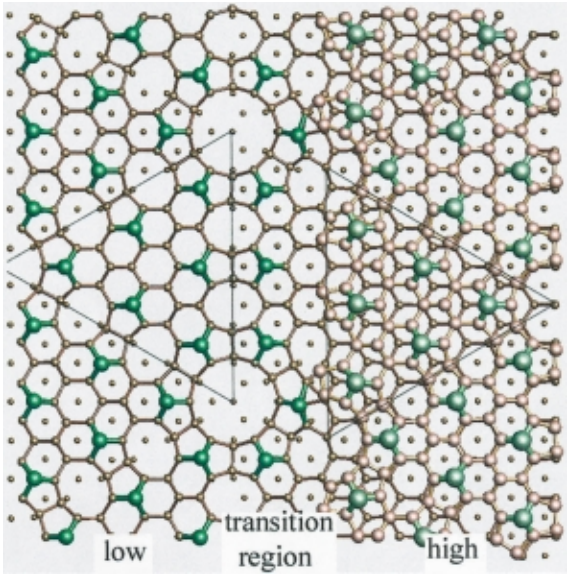

FIG. 2 (color). Schematic presentation of the U2 step configuration based on the STM image. Bonds in two uppermost bilayers and adatom (colored green) layers are shown. The unfaulted subcell with its base parallel to the step is on the high side of the step; the transition region separating the unfaulted subcell on the high side from the faulted subcell on the low side has width 9.1 Å ($n = 2$) and contains four extra adatoms.

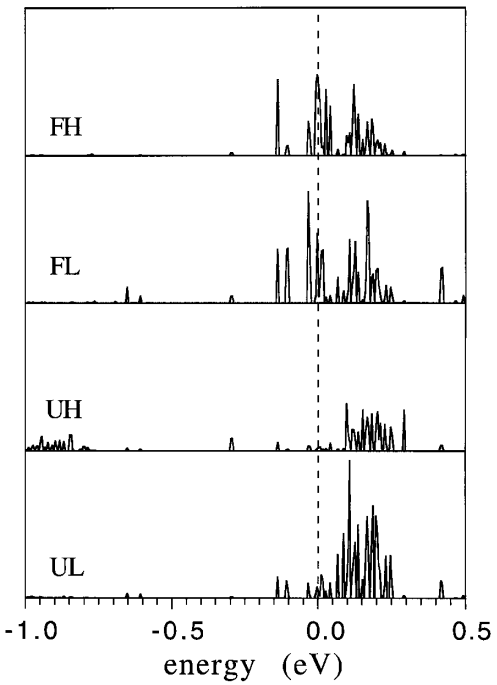

FIG. 3. Local density of states of the adatoms for the p_z tight-binding wave functions for the different subcells adjacent to the U2 step. From top to bottom adatom density of states is shown for the faulted high (FH), the faulted low (FL), the unfaulted high (UH), and the unfaulted low (UL) subcells. The intensity change for the images shown in Figs. 1(a)–1(c) and calculated in Figs. 1(d)–1(f) can be explained from differences in the adatom density of states in the four subcells.

step, except in the narrow transition region where the extra adatoms appear darker.

Using the environment-dependent tight-binding potential the local density of states of the adatoms above and below the Fermi level $E_f = 0$ eV was calculated for the atom configuration shown in Fig. 2. It is plotted in Fig. 3 for the four subcells of the (7×7) unit cell which have one of the sides or vertices close to the step. (The local density of states of the adatoms was also calculated for the two subcells on the flat surface and is different.) Since the states with the higher contribution to the constant height electron maps are the ones that depend strongly on the tip-surface separation, only the density of states that corresponds to the p_z states is shown. (The contribution of the p_x and p_y states to the theoretical maps discussed below was determined from the calculation and was found to be a few percent of the total intensity.) The local density of states of the adatoms shown in Fig. 3 has distinct features both when faulted versus unfaulted subcells are compared (on the same side of the step) or when subcells are compared between the low and the high side of the step. The density of the occupied states (within -0.5 eV below the Fermi level) in the faulted subcell on the low side is larger than the corresponding density of states for the faulted subcell on the high side. The same is true for the adatom density of states of the unfaulted subcells on the low versus the high side of the step. This can explain the higher intensity observed on the low side of the step for $V = -0.5$ V shown in Fig. 1(a). There are larger differences between the local density of states of the adatoms in the faulted and unfaulted subcells on the high versus low side of the step and this explains why the high side of the step has similar contrast between faulted and unfaulted subcells as on the flat surface. When the energy range is increased to 1 eV below the Fermi level new states appear (which are not present on the flat surface) especially within the unfaulted subcell on the high side (i.e., this is a result of the depletion of the adatom density of states close to the Fermi level which enhances the adatom density of states in the energy range well below the Fermi level). This new structure for the adatom density of states -1 eV below the Fermi level reduces the difference of the occupied states above and below the step and can explain the reduced contrast in the image shown in Fig. 1(b). In addition the contrast between faulted and unfaulted subcells on the high side of the step is reduced as a result of the enhancement of the adatom density of occupied states at -1 eV within the unfaulted subcell.

For the energy range above the Fermi level the local density of states of the adatoms is similar in the four subcells. This explains why the images for positive polarity resemble the ones on the flat surface: as shown for $V = +0.25$ V in Fig. 1(c) we see no contrast between subcells on the high and the low side of the step or between faulted versus unfaulted subcells on the same side of the step. Similar images are observed (without contrast

between the low versus the high side of the step or between faulted versus unfaulted subcells at the same side) at other positive voltages. If charge transfer is one of the causes of the adatom intensity difference at negative polarity this does not play a role for positive polarity images which is consistent with the uniform adatom intensity in Fig. 1(c).

In addition to the adatom density of states the calculation gives more information, the detailed dependence of the electron wave function (obtained as a superposition of the atomic wave functions for the Si atoms) on the spatial coordinates x, y, and z. This information can be used to calculate electron density distribution maps at constant value of z which simulates the intensity observed in STM images. The results are shown in Figs. 1(d)–1(f) which correspond to the experimental images obtained for different values of the tunneling voltage -0.5, -1, $+0.25$ V shown to the left. All the wave functions of states within the range from E_f to the value of the tunneling voltage (i.e., below the Fermi level for negative voltages and above the Fermi level for positive voltages) are used to calculate the probability $p(x, y)$ to find an electron at location (x, y) by summing the square of the amplitude of the wave functions within the tunneling range. The darker region observed in the calculated image 1(f) on the high side of the step is a result of the uncertainty in defining the constant height from the step in the calculation of the electron density.

As stated earlier another important feature observed on the flat surface is the reduced intensity of the center adatom (in both the faulted and unfaulted subcells) when images are taken for negative polarity, as a result of charge transfer from the center adatom to the two neighboring rest adatoms. This intensity difference is still seen in all the (7×7) unit cells close and away from the step. In addition the increased number of dangling bonds close to the steps and the presence of the extra atoms in the transition region (for step type U2) provides additional channels for redistributing the electron charge and can result in additional variations of the adatom intensity. Although such measurements are difficult since the intensity variations are, in general, small and require extensive averaging of the adatom intensity in different subcells at the step (and in addition the intensity difference can depend on the sharpness of the tip) we have observed novel, well-reproduced features especially for the adatom intensity on the high side of the step. For example for the three adatoms parallel to the step within the unfaulted subcell on the high side, we have observed that the corner adatom closer to the extra adatom in the transition region on the low side appears brighter than the corner adatom away from the extra adatom. This asymmetry is easily seen experimentally by displaying 1D intensity scans in images 1(a) and 1(b); they can also be seen in the theoretical image 1(d) at -0.5 V (although experimentally it is more pronounced in the -1 V image). One possible explanation of the asymmetry is related to the presence of the extra adatom in the transition region, which limits the proximity and restricts charge transfer of the nearest corner adatom to rest adatoms. The role of charge transfer within the subcells close to the step is currently under detailed investigation.

In summary, we have studied the apparent structure of the two subcells of the (7×7) unit cell close to a step and changes in the adatom intensity as a function of the tunneling voltage. Strong dependence of the subcell contrast is found for tunneling from the occupied states with the subcells on the low side being more intense at $V = -0.5$ V. No intensity contrast was found for tunneling from the unoccupied states. These results are in excellent agreement with the calculated local density of states of the adatoms and the corresponding adatom electron density maps of the (7×7) unit cell close to a step based on an environment-dependent tight-binding model. They confirm the strong correlation between the apparent structure observed in STM images and novel electronic features observed as a result of atom relaxation at steps.

Ames Laboratory is operated for the U.S. Department of Energy by Iowa State University under Contract No. W-7405-eng-82. This work was supported by Director for Energy Research, Office of Basic Energy Sciences and by NATO Grant No. SA.5-2-05(CRG.972214)167197/AHJ-501 (M. H. and M. C. T.).

*Permanent address: Department of Physics, Taegu University, Taegu, Korea.

[1] K. Takayanagi, Y. Tanishiro, M. Takahashi, and S. Takahashi, J. Vac. Sci. Technol. A **3**, 1502 (1985).
[2] R. J. Hamers, R. M. Tromp, and J. E. Demuth, Phys. Rev. Lett. **56**, 1972 (1986).
[3] Z. Zhang, M. A. Kulakov, and B. Bullemer, Surf. Sci. **375**, 195 (1997).
[4] R. Wolkow and Ph. Avouris, Phys. Rev. Lett. **60**, 1049 (1988).
[5] R. S. Becker, J. A. Golovchenko, E. G. McRae, and B. S. Swartzentruber, Phys. Rev. Lett. **55**, 2028 (1985).
[6] J. E. Northup, Phys. Rev. Lett. **57**, 154 (1986).
[7] A. V. Latyshev, A. L. Aseev, H. B. Krasilnikov, and S. I. Stenin, Surf. Sci. **213**, 157 (1989).
[8] C. Z. Wang, B. C. Pan, J. B. Xiang, and K. M. Ho, J. Phys. Condens. Matter **11**, 2043 (1999).
[9] K. M. Ho, A. A. Shvartsburg, B. C. Pan, Y. Z. Lu, C. Z. Wang, J. G. Wacker, J. L. Fye, and F. M. Jarrold, Nature (London) **392**, 582 (1998).
[10] H. Tochihara, W. Shimada, M. Itoh, H. Tanaka, M. Udagawa, and I. Sumita, Phys. Rev. B **45**, 11 332 (1992).
[11] Y. Wang and T. T. Tsong, Phys. Rev. B **53**, 6915 (1996).
[12] J. L. Goldberg *et al.*, J. Vac. Sci. Technol. A **9**, 1868 (1991).
[13] W. Telieps and E. Bauer, Surf. Sci. **162**, 163 (1985).
[14] N. Osakabe, Y. Tanishiro, K. Yagi, and G. Honjo, Surf. Sci. **109**, 353 (1981).